Computationally efficient concentration-based model for accurate evaluation of *T*-junction inlet staggered herringbone micromixers

Nikolaos Vasilakis ✉, *Despina Moschou, Themistoklis Prodromakis*

Nanoelectronics and Nanotechnology Research Group, Southampton Nanofabrication Centre, Electronics and Computer Science, University of Southampton, SO17 1BJ Southampton, UK
✉ *E-mail: n.vasilakis@soton.ac.uk*

Published in Micro & Nano Letters; Received on 6th July 2015; Accepted on 7th January 2016

Micromixers are microfluidic components of critical importance in complex lab-on-chip devices. Passive devices in particular have attracted much attention over active ones due to their fabrication and operation simplicity. Staggered herringbone micromixers seem to be dominating the area of passive micromixers, and hence a lot of studies have been published on their optimisation, in terms of mixing efficiency (ME) and pressure drop. However, numerical simulations leveraging concentration-based models have not been convincingly accurate, owing to computational limitations and erroneous assumptions on diffusion coefficients that often are higher than those of large biomolecules in aqueous solutions. Accurate concentration-based models are a prerequisite in biochemical reaction studies. This work quantitatively shows how increasing mesh density increases solution accuracy, applying concentration-based modelling for biochemically realistic diffusivity. A numerical simulation methodology for obtaining less numerically diffusive results without further increasing mesh size is also given, leveraging quadratic discretisation and appropriate consistency stabilisation methods. They demonstrate that with the proposed approach, it is possible to obtain more accurate ME and pressure drop estimations for two different staggered herringbone micromixer variations, while at the same time limiting the usage of computational resources to a practical level.

1. Introduction: Over the past years, lab-on-chip (LoC) technologies have demonstrated several miniaturisations of existing chemical or biological assays [1–3]. In such microfluidic systems, micromixers are usually incorporated as crucial components [4] for achieving uniform and rapid mixing of reagents and samples [5]. Microscale mixers have to cope with the high surface-to-volume ratio of microchannels, which result in flows within the laminar regime, as opposed to macroscale ones [6, 7]. In particular, the values of the Reynolds number (Re) [8] are below 100 ($\mathrm{Re} < 100$) in case of mediums with kinematic viscosity similar to water and under feasible pressures. As a consequence, the flows are uniaxial and mixing is governed mainly by molecular diffusion. Even though the characteristic length of a conventional straight microchannel is relatively small, the length required for ensuring uniform mixing can be quite long ($\gg 1$ cm) [9].

Micromixers are divided into two types: passive and active. In passive micromixers, no additional energy source is required, apart from pumping energy. The mixing mechanism relies on molecular diffusion or chaotic advection [10]. On the contrary, active micromixers require external energy. Thus, passive micromixers are preferable, owing to their fabrication and integration simplicity in LoC devices, compared with active ones [4].

Stroock *et al.* [9] first proposed and optimised a passive mixing geometry consisting of staggered ridges on the bottom of the channel; nowadays known as staggered herringbone mixer (SHM). This celebrated mixer induces counter rotating vortices across the flow, i.e. chaotic adventive flow, featuring high mixing performance with low pressure drop [11]. SHM can be easily and cost effectively fabricated using standard soft lithography processes [12]. For these reasons, this geometry has been widely used in LoC devices [13–15].

A large volume of simulation studies have focused on evaluating and optimising this particular device [11, 16–20], focusing mainly on water–ethanol solutions or water–glycerol solutions (diffusion coefficient ; 10^{-9} m^2/s) [9, 17, 19–22]. To date, two main variations for modelling have been used: the advection–diffusion within the micromixer: namely, the particle trajectory-based method, and the concentration-based model. Recent studies conclude that the concentration-based model is essential for accurate solutions, particularly in concentration dependent investigations typically required when studying microreactors [23]. The numerical diffusion, however, is often the main drawback of the concentration-based model, requiring a higher mesh resolution for mitigating this issue; overall a rather computationally demanding solution.

In this Letter, we propose an optimal method to mitigate the numerical diffusion effect of concentration-based model by using COMSOL Multiphysics®, resulting in a dramatic decrease in computational resources. Coarse meshing, second-order discretisation of the concentration terms in the mass balance equation and Codina cross-wind stabilisation technique were applied to that end. The mixing efficiency (ME) of distinct SHM designs was investigated for diluted large biomolecules in water-based solutions, utilising a more realistic diffusion coefficient (diffusion coefficient ; 10^{-11} m^2/s) [6, 11].

2. Numerical model: All simulations were performed utilising the COMSOL Multiphysics® software package. High-memory computational nodes of the University of Southampton Supercomputing facility Iridis 4 were leveraged. Each employed node consisted of 32 cores (2.6 GHz) and 256 GB of random access memory (RAM) [24].

We first simulated the archetypical SHM passive micromixing structure (Fig. 1*a*) proposed by Stroock *et al.* [9]. The presented topology induces transverse flows along the microchannel, where the molecules of the medium follow helical shaped streamlines [6]. This chaotic adventive mixing design is based on staggered ridges at the bottom of the channel. For flow-through microfluidic channels featuring large biological molecules in aqueous solutions, the Peclet number typically ranges between 100 and 10.000 [6]. Therefore, chaotic advection is ideal for a laminar flow condition in micromixers, rendering SHM an ideal geometry.

The two inlets of the mixer (100 µm wide and 150 µm tall) form a *T*-junction driving the medium into the main SHM (channel width $w = 200$ µm and channel height $h = 150$ µm), as illustrated in Fig. 1*b*. The mixer comprises 25 ridges lying at the bottom of the

doi: 10.1049/mnl.2015.0239

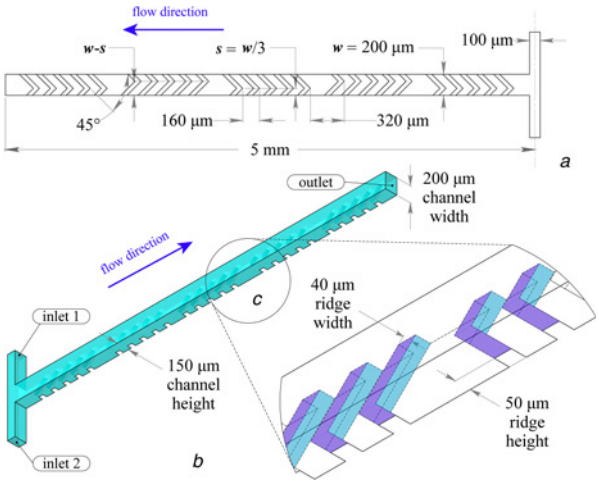

Fig. 1 *SHM design*
a Top view
b Isometric view
c Ridges detail

channel that are divided into five alternating groups with respect to the centreline of the channel. The distance between the groups is 320 μm, as illustrated in Fig. 1*a*. Every group consists of five staggered herringbone ridges, spaced at 160 μm from each other. Each herringbone comprises of two arms, forming a 45° angle with respect to the centreline of the channel. The minimum distance between the apex of the ridges and the sidewall determines the asymmetry index $\boldsymbol{s}$ of the geometry, as illustrated in Fig. 1*a*, and is defined as a fraction to the channel width $\boldsymbol{w}$. Each ridge is 40 μm wide and 50 μm deep (Fig. 1*c*).

A laminar incompressible steady-state flow model was employed since the studied volumetric flow rates along the microchannel are between 18 and 360 μl/min. The medium flowing through the channel via both inlets is considered to be water at 20°C. Considering the kinematic viscosity of the fluid such flow rates lead to flows with a Reynolds number within the laminar range (Re = 2000). In particular, all simulated flow rates through an identical dimension model microfluidic channel that does not have any ridges result in Re < 100. The applied model consists of the mass and momentum conservation equations, as shown in (1) and (2), for steady-state incompressible flow where gravitational effects are neglected

$$\nabla \cdot \boldsymbol{u} = 0 \tag{1}$$

$$(\boldsymbol{u} \cdot \nabla)\boldsymbol{u} = -\frac{\nabla p}{\rho} + \nu \nabla^2 \boldsymbol{u} \tag{2}$$

where $\boldsymbol{u}$ is the velocity vector, p is the pressure, ρ is the density of the medium and ν is the kinematic viscosity [25].

A parabolic velocity profile of fully developed laminar flow was defined over the two inlets. No-slip velocity on the channel walls was further applied as a boundary condition. The micromixing topologies were numerically investigated for the following flow rates: 18, 90, 180 and 360 μl/min. The laminar flow equations were discretised by first-order elements over a proper hexahedral mesh to achieve accurate and grid-independent solutions.

The transport of diluted species module of COMSOL Multiphysics® is a concentration-based advection–diffusion model. The concentrations of diluted species over inlets 1 and 2 were considered as 1 and 0 mol/m^3, respectively, i.e. $C_1 = 1$ mol/m^3 and $C_2 = 0$ mol/m^3. In the case of steady state, the implemented mass balance equation of the model is

$$\boldsymbol{u} \cdot \nabla C = \nabla \cdot (D \nabla C) \tag{3}$$

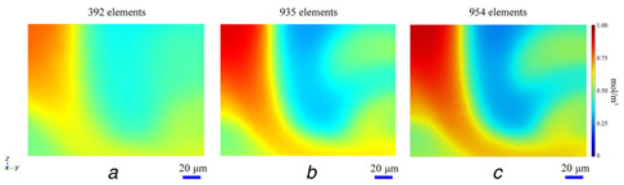

Fig. 2 *Concentration of diluted species on the outflow surface of SHM design with a = w/4 for different mesh density*
a 392 Elements over the outflow surface, ME$_a$ = 0.79
b 935 Elements over the outflow surface, ME$_b$ = 0.67
c 954 Elements over the outflow surface, ME$_c$ = 0.63

where $\boldsymbol{u}$ is the velocity vector of the solvent, C is the concentration of the diluted species and D is the diffusion coefficient of the diluted species in the solvent. Large biological molecules in water have a diffusion coefficient in the order of 10^{-11} m^2/s [6, 26]. In this Letter, we assumed a diffusion coefficient of 5×10^{-11} m^2/s.

As the main drawback of the concentration-based modelling is the artificial numerical diffusion, we studied two different discretisation types of the concentration in the mass balance equation: namely, the linear and the quadratic. Additionally, we investigated the two different stabilisation techniques for the cross-wind diffusion method: namely, the Da Carmo – Galeao and the Codina. The Codina formulation is considered less diffusive compared with the Da Carmo – Galeao [27].

The ME and pressure drop (ΔP) were calculated to assess the micromixers [21]. The ME is an expression of the standard deviation of the diluted species over a number of computational nodes. In this Letter, the ME has been calculated over the nodes of the outflow surface. The mathematical expression of the ME is presented in (4)

$$\mathrm{ME} = 1 - \sqrt{\frac{1}{N}\sum_{i=1}^{N}\left(\frac{C_i - \bar{C}}{\bar{C}}\right)^2} \tag{4}$$

where $\bar{C}$ is the concentration of fully mixed medium (in our case 0.5 mol/m^3), C_i is the concentration on a given position (spatial discretisation point) and N is the total number of discretisation points over the outflow surface.

3. Results and discussion: We begin by simulating an SHM (Fig. 1) with an asymmetry index $\boldsymbol{s} = \boldsymbol{w}/4$, the volumetric flow rate being constant at 18 μl/min. The value of $\boldsymbol{s}$ was chosen over the optimum position of the ridges ($\boldsymbol{s} = \boldsymbol{w}/3$), aiming at a lower ME, so that the numerical artificial diffusion becomes conspicuous.

The concentration-based model exhibits high dependence on mesh density [23]. As Fig. 2 depicts, in case of linear discretisation of species concentration (first-order elements), the calculated ME over the outflow surface depends on the total number of elements. The coarse mesh of the model presented in Fig. 2*a* generates a high numerical diffusion, causing an overestimation in ME (ME$_a$ = 0.79). After refinement of the mesh used in the advection–diffusion model, the total number of elements over the outflow surface increases causing a significant decrease in the numerical diffusion (ME$_b$ = 0.67). Refining even further the mesh, we only get a slightly decreased estimation of ME$_c$ = 0.63 (Fig. 2*c*). The calculated ME over the outflow surface presented in Fig. 2*a* is overestimated by 25% compared with the achieved solution in Fig. 2*c* (ME$_c$ = 0.63). In all of these results, the Da Carmo – Galeao consistency stabilisation method was employed, with first-order elements (linear).

As revealed in Fig. 3, the ME is highly dependent on mesh density and it is apparent that the total number of elements on the outflow surface should be increased. However, further refinement of the mesh toward achieving a grid-independent solution would

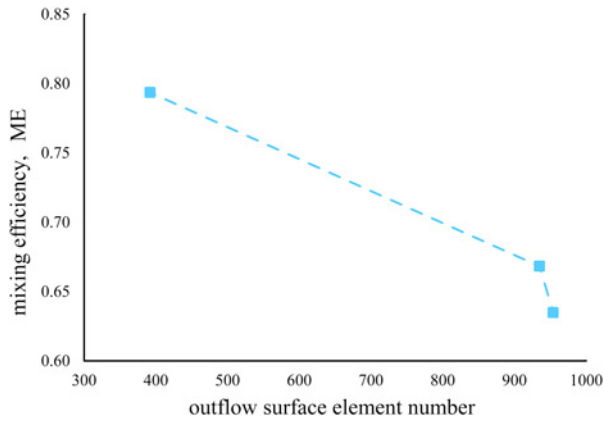

Fig. 3 *ME plotted against the total number of elements over the outflow surface*

overall render a more computationally intensive solution. It is notable that the model presented in Fig. 2*c* required 206 GB of RAM and more than 11 h to achieve convergence.

To alleviate this challenge, we studied the increase of the element order from linear (Fig. 4*a*, also presented previously as Fig. 2*c* for ease of comparison) to quadratic (Fig. 4*b*). A coarser mesh was utilised for the spatial discretisation of the design, combined however with the Codina stabilisation technique for the cross-wind diffusion method, being less numerically diffusive [27, 28]. These discretisation parameters resulted in a lower total number of elements (~17 times lower) for the concentration-based model as compared with the dense mesh shown in Fig. 4*a*. Subsequently, the outflow surface elements decreased from 954 to 811, allowing for a 14% decrease. Moreover, the required computation power decreased remarkably to a total computational time of 30 min and a 25 GB RAM utilisation.

The computationally efficient solution illustrated in Fig. 4*b* results in an ME of 0.40, whereas the more dense and computationally demanding model (Fig. 4*a*) results in ME = 0.63. By observing Figs. 4*a* and *b*, it is obvious that Fig. 4*b* constitutes a less numerically diffusive result than Fig. 4*a* and consequently more accurate.

Hence, this approach offers a more accurate ME estimation at a lower computational time (23 times) and RAM utilisation (8 times) from the aforementioned linear discretisation approach.

To further validate this optimised concentration-based model, two distinct SHM designs that employed different asymmetry indexes ($s = w/3$ and $s = w/4$) were simulated for four volumetric flow rates (Fig. 5) and their concentration distributions were calculated. All the boundary conditions (no-slip velocity, parabolic velocity profiles over the inlets, C_1, C_2, D etc.) taken into account

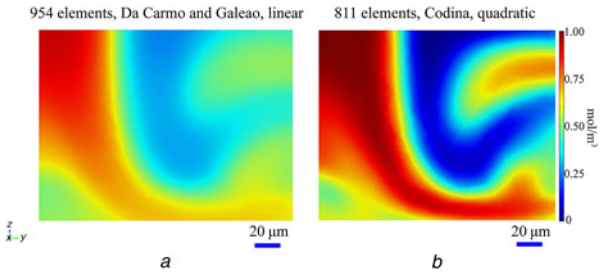

Fig. 4 *Comparison of the discretisation method and the consistency stabilisation method for the cross-wind diffusion of the transport of diluted species module*
a Dense mesh (31.1×10^6 total elements) with Da Carmo – Galeao consistency stabilisation method and linear discretisation (ME = 0.63)
b Coarse mesh (1.78×10^6 total elements) with Codina consistency stabilisation method and quadratic discretisation method (ME = 0.40)

are the same for both designs. Fig. 5 is separated in two columns, *a* and *b* demonstrating results for $s = w/3$ and $s = w/4$, respectively.

Fig. 5*a* presents a more uniform concentration distribution compared with Fig. 5*b* for every different volumetric flow rate. Our findings are consistent with those of Stroock *et al.* [9], who suggested that the optimum asymmetry index for the SHM designs is $s = w/3$, as well as with Cortes-Quiroz *et al.* [20] numerical confirmations.

The bar chart shown in Fig. 6 summarises the calculated ME over the outflow surface for every simulated volumetric flow rate. Stripped bars represent $s = w/3$ and solid ones $s = w/4$. The calculated pressure drop along the SHM is almost identical for both studied s; hence the reported ΔP is common for both simulated designs at each volumetric flow rate.

By changing the asymmetry parameter s from $w/4$ to $w/3$, a significant improvement of the ME (75% increase) was observed for a low volumetric flow rate (18 μl/min). For higher volumetric flow rates, s has a lower impact (23%), but still remains significant. Thus, the ME of both proposed designs indicates an increase with increasing volumetric flow rate. However, the SHM mixer has been shown to exhibit a decreasing ME with increasing volumetric

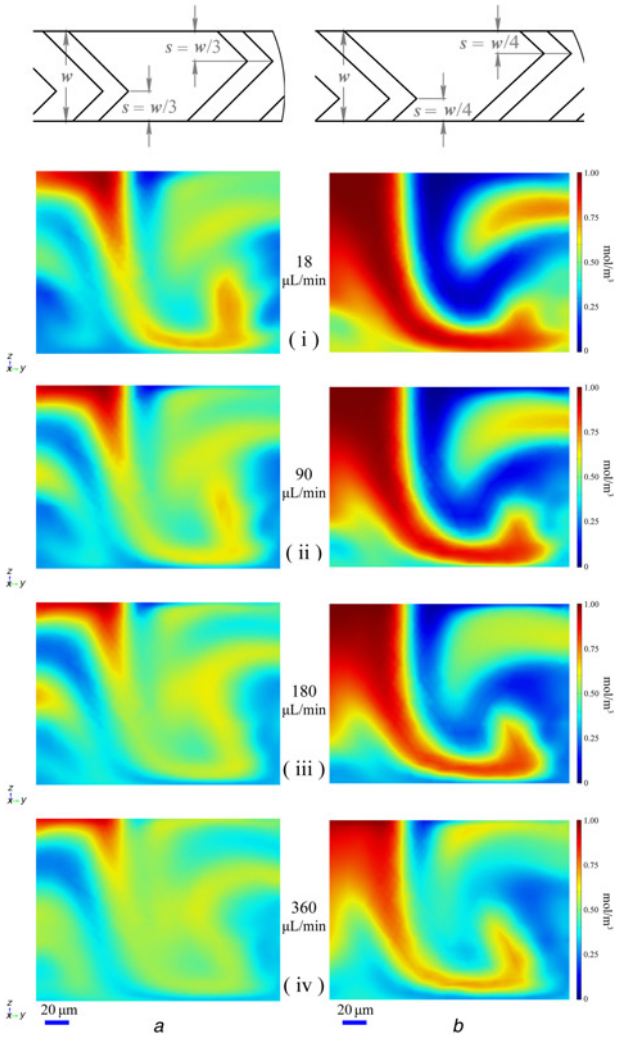

Fig. 5 *Concentration distribution over the outflow surface of two different design variations*
a $s = w/3$
b $s = w/4$
and under increasing volumetric flow rates q
i $q = 18$ μl/min
ii $q = 90$ μl/min
iii $q = 180$ μl/min
iv $q = 360$ μl/min

doi: 10.1049/mnl.2015.0239

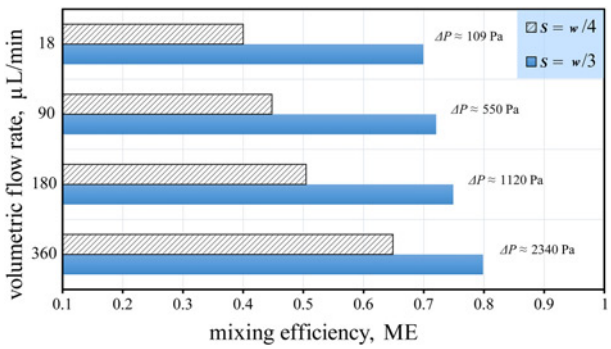

Fig. 6 *Bar chart presenting the ME against the volumetric flow rate*

flow rate [9]. This difference could be ascribed to the fact that in our simulated geometry the herringbone structures are formed as ridges occupying 1/3 of channel height, as opposed to grooves embedded in the channel [9]. Additionally, the combination of the particular structure with the *T*-junction inlet seems to enhance the induced chaotic advection.

4. Conclusions: Optimisation of staggered herringbone micromixing as components in complex LoC devices is a field of great research interest. Convincing simulation accuracy however is yet to be achieved due to the high computational resources required to successfully incorporate the concentration-based model. This Letter confirms via COMSOL Multiphysics® v4.4 that the weakness of the concentration-based model is numerical diffusion. High-density spatial discretisation with first-order elements can reduce numerical diffusion, but leads to computationally demanding models. Evidence from the present Letter suggests that a coarse mesh can be combined with second-order elements (quadratic). In addition, the Codina stabilisation technique might be used to lower the numerical diffusion. This proposed method could mitigate the utilised computational resources (23 times shorter computational time and 8 times lower RAM usage), while an accurate solution of the ME of the micromixing topology is achieved. Utilising our suggested simulation approach, we concluded that the *T*-junction inlet SHM has an outstanding mixing performance for large biomolecules diluted in aqueous solutions (diffusion coefficient $\simeq 10^{-11}$ m^2/s) with almost the same pressure drop regardless of the topology's asymmetry index. Finally, the proposed mixing design appears to achieve higher ME by increasing the volumetric flow rate.

5. Acknowledgments: The authors wish to acknowledge the financial support of the A.G. Leventis Foundation and EPSRC EP/L020920/1.

6 References

[1] Moschou D., Vourdas N., Filippidou M.K., *ET AL.*: 'Integrated biochip for PCR-based DNA amplification and detection on capacitive biosensors', *Bio-Mems Med. Microdevices*, 2013, **8765**, pp. 87650L-1-9
[2] Haeberle S., Zengerle R.: 'Microfluidic platforms for lab-on-a-chip applications', *Lab Chip*, 2007, **7**, (9), pp. 1094–1110
[3] Foudeh A.M., Fatanat Didar T., Veres T., *ET AL.*: 'Microfluidic designs and techniques using lab-on-a-chip devices for pathogen detection for point-of-care diagnostics', *Lab. Chip*, 2012, **12**, (18), pp. 3249–3266
[4] Mansur E.A., Ye M.X., Wang Y.D., *ET AL.*: 'A state-of-the-art review of mixing in microfluidic mixers', *Chin. J. Chem. Eng.*, 2008, **16**, (4), pp. 503–516
[5] Lee C.Y., Chang C.L., Wang Y.N., *ET AL.*: 'Microfluidic mixing: a review', *Int. J. Mol. Sci.*, 2011, **12**, (5), pp. 3263–3287
[6] Nguyen N.-T.: 'Micromixers: fundamentals, design and fabrication' (William Andrew, New York, USA, 2012, 2nd edn.)
[7] Beebe D.J., Mensing G.A., Walker G.M.: 'Physics and applications of microfluidics in biology', *Annu. Rev. Biomed. Eng.*, 2002, **4**, pp. 261–286
[8] White F.M.: 'Fluid mechanics' (McGraw-Hill, New York, USA, 2011, 7th edn.)
[9] Stroock A.D., Dertinger S.K., Ajdari A., *ET AL.*: 'Chaotic mixer for microchannels', *Science*, 2002, **295**, (5555), pp. 647–651
[10] Capretto L., Cheng W., Hill M., *ET AL.*: 'Micromixing within microfluidic devices', *Topics Curr. Chem.*, 2011, **304**, pp. 27–68
[11] Kee S.P., Gavriilidis A.: 'Design and characterisation of the staggered herringbone mixer', *Chem. Eng. J.*, 2008, **142**, (1), pp. 109–121
[12] Xia Y.N., Whitesides G.M.: 'Soft lithography', *Annu. Rev. Mater. Sci.*, 1998, **28**, pp. 153–184
[13] Hessel V., Lowe H., Schonfeld F.: 'Micromixers – a review on passive and active mixing principles', *Chem. Eng. Sci.*, 2005, **60**, (8–9), pp. 2479–2501
[14] Williams M.S., Longmuir K.J., Yager P.: 'A practical guide to the staggered herringbone mixer', *Lab Chip*, 2008, **8**, (7), pp. 1121–1129
[15] Park D.S., Egnatchik R.A., Bordelon H., *ET AL.*: 'Microfluidic mixing for sperm activation and motility analysis of Pearl Danio Zebrafish', *Theriogenology*, 2012, **78**, (2), pp. 334–344
[16] Du Y., Zhang Z.Y., Yim C., *ET AL.*: 'A simplified design of the staggered herringbone micromixer for practical applications', *Biomicrofluidics*, 2010, **4**, (2), pp. 024105-1-13
[17] Hossain S., Husain A., Kim K.Y.: 'Shape optimization of a micromixer with staggered-herringbone grooves patterned on opposite walls', *Chem. Eng. J.*, 2010, **162**, (2), pp. 730–737
[18] Aubin J., Fletcher D.F., Xuereb C.: 'Design of micromixers using CFD modelling', *Chem. Eng. Sci.*, 2005, **60**, (8–9), pp. 2503–2516
[19] Fodor P.S., Itomlenskis M., Kaufman M.: 'Assessment of mixing in passive microchannels with fractal surface patterning', *Eur. Phys. J. Appl. Phys.*, 2009, **47**, (3), pp. 31301-1-8
[20] Cortes-Quiroz C.A., Zangeneh M., Goto A.: 'On multi-objective optimization of geometry of staggered herringbone micromixer', *Microfluidics Nanofluidics*, 2009, **7**, (1), pp. 29–43
[21] Solehati N., Bae J., Sasmito A.P.: 'Numerical investigation of mixing performance in microchannel T-junction with wavy structure', *Comput. Fluids*, 2014, **96**, pp. 10–19
[22] Ansari M.A., Kim K.Y.: 'Shape optimization of a micromixer with staggered herringbone groove', *Chem. Eng. Sci.*, 2007, **62**, (23), pp. 6687–6695
[23] Toth E.L., Holczer E.G., Ivan K., *ET AL.*: 'Optimized simulation and validation of particle advection in asymmetric staggered herringbone type micromixers', *Micromachines*, 2015, **6**, (1), pp. 136–150
[24] http://cmg.soton.ac.uk/iridis, accessed date
[25] Munson B.R., Okiishi T.H., Huebsch W.W., *ET AL.*: 'Fundamentals of fluid mechanics' (John Wiley & Sons, Inc., New Jersey, USA, 2013, 7th edn.)
[26] Papadopoulos V.E., Kefala I.N., Kaprou G., *ET AL.*: 'A passive micromixer for enzymatic digestion of DNA', *Microelectron. Eng.*, 2014, **124**, pp. 42–46
[27] http://www.comsol.com/blogs/understanding-stabilization-methods/, accessed date 2014
[28] Codina R.: 'A discontinuity-capturing crosswind-dissipation for the finite-element solution of the convection-diffusion equation', *Comput. Methods Appl. Mech. Eng.*, 1993, **110**, (3–4), pp. 325–342